High precision measurements of the ground state hyperfine structure interval of muonium and of the muon magnetic moment

W Liu, M G Boshier, S Dhawan, O van Dyck, P Egan, X Fei, M Grosse Perdekamp, V W Hughes, M Janousch, K Jungmann, D Kawall, F G Mariam, C Pillai, R Prigl, G zu Putlitz, I Reinhard, W Schwarz, P A Thompson, K A Woodle

High Precision Measurements of the Ground State Hyperfine Structure Interval of Muonium and of the Muon Magnetic Moment

W. Liu,[1] M. G. Boshier,[1] S. Dhawan,[1] O. van Dyck,[2] P. Egan,[3] X. Fei,[1] M. Grosse Perdekamp,[1] V. W. Hughes,[1]
M. Janousch,[1,4] K. Jungmann,[5] D. Kawall,[1] F. G. Mariam,[6] C. Pillai,[2] R. Prigl,[1,6] G. zu Putlitz,[5] I. Reinhard,[5]
W. Schwarz,[1,5] P. A. Thompson,[6] and K. A. Woodle[6]

[1]*Department of Physics, Yale University, New Haven, Connecticut 06520-8121*
[2]*Los Alamos National Laboratory, Los Alamos, New Mexico 87545*
[3]*Lawrence Livermore National Laboratory, Livermore, California 94550*
[4]*ETH Zürich, Institute for Particle Physics, CH-5232 Villigen-PSI, Switzerland*
[5]*Universität Heidelberg, Physikalisches Institut, D-69120 Heidelberg, Germany*
[6]*Brookhaven National Laboratory, Upton, New York 11973*
(Received 21 August 1998)

High precision measurements of two Zeeman hyperfine transitions in the ground state of muonium in a strong magnetic field have been made at LAMPF using microwave magnetic resonance spectroscopy and a resonance line narrowing technique. These determine the most precise values of the ground state hyperfine structure interval of muonium $\Delta\nu = 4\,463\,302\,765(53)$ Hz (12 ppb), and of the ratio of magnetic moments $\mu_\mu/\mu_p = 3.183\,345\,13(39)$ (120 ppb), representing a factor of 3 improvement. Values of the mass ratio m_μ/m_e and the fine structure constant α are derived from these results.
[S0031-9007(98)08281-7]

PACS numbers: 36.10.Dr, 12.20.Fv

Muonium ($\mu^+ e^-$, M) is the hydrogenlike bound state of a positive muon and an electron. However, unlike for hydrogen, theoretical predictions of its ground state hyperfine structure can be obtained with high precision since the complications of proton structure are absent. This enables a most sensitive test of two-body bound state QED to be made, with the assumption of $e - \mu$ universality. Hyperfine transition measurements may also be used to extract the fundamental constants μ_μ/μ_p and m_μ/m_e. In addition, using the theory, the fine structure constant α can be determined and used to test the internal consistency of QED through comparison with α determined from the electron anomalous g factor, a_e.

In a static magnetic field the muonium ground state $1^2S_{1/2}$ energy levels are described by the Hamiltonian [1]

$$\mathcal{H} = h\Delta\nu \mathbf{I}_\mu \cdot \mathbf{J} - \mu_B^\mu g'_\mu \mathbf{I}_\mu \cdot \mathbf{H} + \mu_B^e g_J \mathbf{J} \cdot \mathbf{H}, \quad (1)$$

where $\mathbf{I}_\mu$ is the muon spin operator, $\mathbf{J}$ is the electron total angular momentum operator, $\mathbf{H}$ is the external static magnetic field, and the muon (electron) Bohr magneton is denoted by $\mu_B^\mu (\mu_B^e)$. The gyromagnetic ratios of an electron bound in muonium, g_J, and of a muon in muonium, g'_μ, differ from the free values, g_e and g_μ, by binding corrections [2]

$$g_J = g_e \left(1 - \frac{\alpha^2}{3} + \frac{\alpha^2}{2} \frac{m_e}{m_\mu} + \frac{\alpha^3}{4\pi} \right), \quad (2)$$

$$g'_\mu = g_\mu \left(1 - \frac{\alpha^2}{3} + \frac{\alpha^2}{2} \frac{m_e}{m_\mu} \right). \quad (3)$$

In a strong field the ground state splits into four substates defined by the magnetic quantum numbers (M_J, M_μ), and the transitions for $(1/2, 1/2) \leftrightarrow$ $(1/2, -1/2)$ designated ν_{12}, and $(-1/2, -1/2) \leftrightarrow$ $(-1/2, 1/2)$ designated ν_{34}, are observed by a microwave magnetic resonance technique. The transition frequencies based on (1) are given by the Breit-Rabi formula [1]

$$\nu_{12} = -\frac{\mu_B^\mu g'_\mu H}{h} + \frac{\Delta\nu}{2}[(1 + x) - \sqrt{1 + x^2}], \quad (4)$$

$$\nu_{34} = +\frac{\mu_B^\mu g'_\mu H}{h} + \frac{\Delta\nu}{2}[(1 - x) + \sqrt{1 + x^2}], \quad (5)$$

where $x = (g_J \mu_B^e + g'_\mu \mu_B^\mu)H/(h\Delta\nu)$ is proportional to the magnetic field strength, H. We use the Larmor relation, $2\mu_p H = h\nu_p$, and NMR to determine H in terms of the free proton precession frequency, ν_p, and the proton magnetic moment, μ_p. Then using (4), (5), and measurements of the transition frequencies ν_{12} and ν_{34}, we extract $\Delta\nu$ and μ_μ/μ_p for positive muons [3].

The muons for the experiment were derived from the linear accelerator at the Clinton P. Anderson Meson Physics Facility (LAMPF) at Los Alamos, which produced an 800 MeV proton beam in 650 μs pulses at 120 Hz. Interactions of the proton beam with a graphite target produced many π^+, whose parity violating decay at rest near the surface of the target yielded negative helicity μ^+. These were transported to the experimental apparatus by the stopped muon channel (SMC) [4], which was tuned to accept μ^+ of 28 MeV/c which were nearly 100% polarized, had a FWHM $\Delta p/p$ of 10%, and yielded an average intensity of a few $\times 10^7$ μ^+/s. Impurities in the beam were reduced by gas barriers and an $\mathbf{E} \times \mathbf{H}$ separator which reduced the ratio e^+/μ^+ in the beam from about 10 to 0.03 [5].

At the end of the SMC, the muons entered the bore of a large superconducting solenoidal MRI magnet at a field of 1.7 T. Centered in the solenoid was a copper pillbox microwave cavity containing either 0.8 or 1.5 atm of 99.97% pure krypton gas, with an O_2 content <5 ppm (ppm: parts per 10^6). Collisions in the gas slowed the muons, which stopped and formed polarized muonium predominantly in the $(1/2, -1/2)$ and $(-1/2, -1/2)$ states through the spin-preserving electron capture reaction $\mu^+ + Kr \rightarrow \mu^+ e^- + Kr^+$ [1]. With the time constant of the muon lifetime, $\tau_\mu = 2.197\,03(4)$ μs [6], the muons would decay weakly via $\mu^+ \rightarrow e^+ + \nu_e + \bar{\nu}_\mu$, where the momentum and angle of the decay e^+ are functions of the muon polarization. Since high momenta decay positrons are emitted preferentially in the direction of the muon spin, by driving the ν_{12} and ν_{34} transitions with an applied microwave magnetic field perpendicular to the static field **H**, the muon spin could be flipped and the angular distribution of high momenta positrons changed from predominantly upstream to downstream with respect to the beam direction [1]. An aluminum endcap and polyethylene absorber downstream of the cavity absorbed positrons with energies below 35 MeV, followed by two scintillators operated in coincidence to detect the high momenta decay e^+.

We define the signal, $S(\nu, H) = (N_{on}/N_{off} - 1)$, where N_{on} is the number of positrons detected downstream of the microwave cavity with an applied microwave magnetic field of frequency ν in a magnetic field of strength H, and N_{off} the number with no applied microwave field. Close to resonance, S becomes large and positive. In practice, the number of detected positrons was normalized to the number of incident muons, whose flux and profile were monitored with a thin plastic scintillator and wire chamber upstream of the microwave cavity. A schematic of the apparatus is shown in Fig. 1.

The cavity was designed to be resonant simultaneously in the TM_{110} mode at the ν_{12} transition frequency of about 1897.5 MHz, and in the TM_{210} mode at the ν_{34} frequency of roughly 2565.8 MHz. In a typical resonance line scan, one mode of the cavity was excited for 10 cycles of the

proton beam and N_{on} counts were accumulated, then for 10 cycles the microwave field was turned off and N_{off} was measured. In the next 20 cycles the other transition was measured.

Resonance curves were obtained using two techniques. In the magnetic field sweep of the resonance lines at fixed microwave frequency, data were taken at a particular field for 10 sec, then the current of a 69 cm bore normal conducting modulation coil was increased or decreased. About 120 steps were used to change H by ± 0.005 T about a central field of 1.7 T, with each step corresponding to a change in the microwave transition frequency of about 3.2 kHz. Using small steps reduced the field measurement error associated with induced currents. In the microwave frequency sweep at fixed magnetic field strength, 20 steps of about 20 kHz were made while quartz tuning bars located inside the krypton gas target were moved to keep the cavity in tune.

It was important to measure and stabilize all variables which affect the center and shape of the resonance curves. The magnetic field provided by the solenoid was stable to 1 part in 10^7 to 10^8 per hour, with a peak to peak inhomogeneity of ≤ 1 ppm over the volume in which muonium was formed. A pulsed NMR magnetometer [7] with eight probes measured the field outside the cavity several times per second in terms of the free induction decay precession frequency of protons in a zero susceptibility $H_2O + NiCl_2$ ($\sim$ 015 Mol/l) solution. A radially movable NMR probe determined the relation of the field outside to the inside of the cavity. Finally, the NMR frequency of the movable probe was related to the equivalent free proton precession frequency by comparison with an absolute calibration probe [8] containing a spherical water sample for which the dominant shielding and susceptibility corrections, including those from air, have been made. This allowed the absolute field at each point to be known to $\simeq 0.1$ ppm. Another important experimental variable was the microwave power which was actively stabilized to $\leq 7 \times 10^{-4}$ across a line. Typically 3–5 watts of microwave power were used, where the Q of the cavity was 14 000 at the ν_{12} frequency in the TM_{110} mode, and 19 000 at ν_{34} in the TM_{210} mode. The temperature of the krypton gas target was monitored with thermocouples and RTD sensors to a precision of 0.2 °C, and was stable within 0.1 °C. The gas pressure was measured by a Mensor gauge to a precision of $\sim 5 \times 10^{-4}$ atm. Finally, because the magnetic field was not perfectly homogeneous, each volume element in the cavity had a slightly different resonance line center. In order to weight each element correctly, the stopped muons spatial distribution was obtained with a planar wire chamber.

A major improvement of this experiment over the earlier work [9] is the use of a resonance line narrowing technique [10]. In the conventional approach, the signal, S, is obtained by counting positrons throughout the beam-on time. In terms of the muon lifetime, τ_μ, and the square
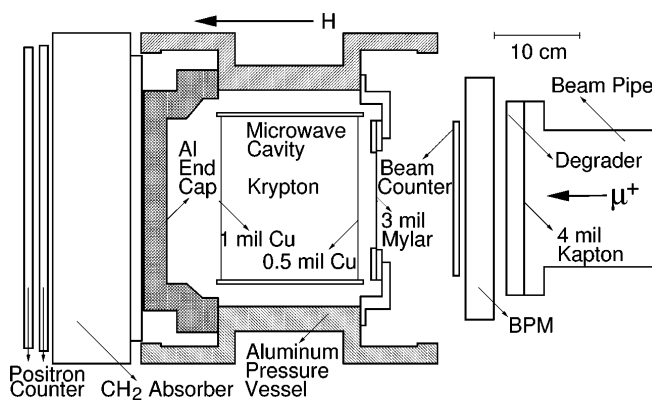

FIG. 1. A schematic of the experimental apparatus.

of the transition matrix element, $|b_{ij}|^2$, the signal shape is roughly described by

$$S \sim \frac{2|b_{ij}|^2}{4\pi^2(\nu_{ij} - \nu)^2 + 4|b_{ij}|^2 + 1/\tau_\mu^2}, \quad (6)$$

where ν_{ij} ($ij = 12, 34$) is the transition frequency and ν is the applied microwave magnetic field frequency. In the limit of zero microwave power ($|b_{ij}|^2 \to 0$) the linewidth $\simeq 1/(\pi\tau_\mu) = 145$ kHz. Observing "old muonium" atoms which have lived several times longer than τ_μ while interacting coherently with the microwave magnetic field results in narrower lines with larger signal amplitude. This was achieved through the use of an **E** field chopper [5] which modulated the μ^+ beam with a 4 μs beam-on period followed by a 10 μs beam-off period, during which the beam was nearly 99% extinguished. Decay positron counts were accumulated in eleven 0.95 μs wide windows, with each successive window observing increasingly old muonium atoms. Lines narrower than the conventional linewidth by a factor of 3 were observed, as were significantly larger signal amplitudes. Both features compensated the reduction in counting rate and reduced some systematic errors.

The centers of the resonance curves were determined by fitting a theoretical resonance line shape [10,11] to the data. The theoretical signal incorporated the measured magnetic field distribution, the ideal microwave power distributions, the muon stopping distribution, the solid angle for detection of an e^+ from μ^+ decay, the effects of the residual unchopped beam, and integrals over the duration of the muon pulse and volume in which muonium was formed. In total, about 200 conventional resonance lines and 1070 old muonium lines were analyzed (see Fig. 2). The χ^2 distributions of the fits indicated good agreement between the theoretical line shape and the experimental data. The transition frequencies resulting from the fits were then transformed to their values in a magnetic field strength corresponding to a free proton precession frequency of 72.320 000 MHz. The data were taken at 0.8 and 1.5 atm, and so were corrected for a small quadratic pressure shift [9,12] and then extrapolated linearly to zero pressure to obtain $\Delta\nu$ and μ_μ/μ_p. The results obtained from each sweeping method were consistent, and were combined to yield our final results

$$\nu_{12}(\text{exp}) = 1\,897\,539\,800(35) \text{ Hz} \quad (18 \text{ ppb}), \quad (7)$$

$$\nu_{34}(\text{exp}) = 2\,565\,762\,965(43) \text{ Hz} \quad (17 \text{ ppb}), \quad (8)$$

$$\Delta\nu(\text{exp}) = 4\,463\,302\,765(53) \text{ Hz} \quad (12 \text{ ppb}), \quad (9)$$

$$\mu_\mu/\mu_p = 3.183\,345\,13(39) \quad (120 \text{ ppb}), \quad (10)$$

where the linear correlation coefficient of ν_{12} and ν_{34} is -0.073 and that of μ_μ/μ_p and $\Delta\nu$ is 0.11. The sources of uncertainty in the results, primarily statistical, are outlined in Table I (ppb: parts per 10^9).
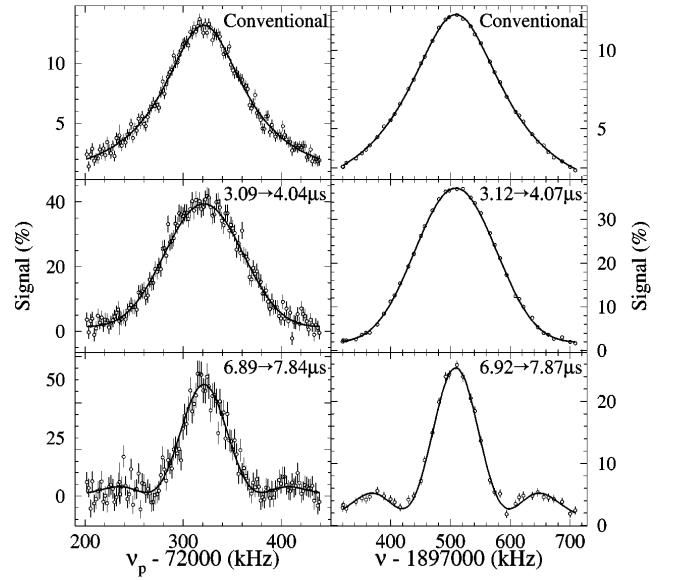

FIG. 2. Resonance curves obtained by sweeping the magnetic field using a conventional method, and from different time windows after muonium production are shown on the left. Microwave frequency sweep curves are on the right. The solid curves are fits to the theoretical line shape [10,11].

Interest in these results stems from their use in making precision tests of QED and for extracting fundamental constants. To this end, we combine (9) and (10) with the results of the last precision experiment [9] to obtain

$$\Delta\nu(\text{exp}) = 4\,463\,302\,776(51) \text{ Hz} \quad (11 \text{ ppb}), \quad (11)$$

$$\mu_\mu/\mu_p = 3.183\,345\,24(37) \quad (120 \text{ ppb}). \quad (12)$$

A precise value for the ratio m_μ/m_e can be obtained from (12) through the relation

$$\frac{m_\mu}{m_e} = \left(\frac{g_\mu}{2}\right)\left(\frac{\mu_p}{\mu_\mu}\right)\left(\frac{\mu_B^e}{\mu_p}\right)$$

$$= 206.768\,277(24) \quad (120 \text{ ppb}), \quad (13)$$

where we have used μ_μ/μ_p from (12), $g_\mu = 2(1 + a_\mu)$ where $a_\mu = 1\,165\,923(8.5) \times 10^{-9}$ [13], and $\mu_p/\mu_B^e = 1.521\,032\,202(15) \times 10^{-3}$ [14].

To test QED requires a theoretical prediction for $\Delta\nu$, which is described in leading order by the Fermi formula

$$\Delta\nu(\text{Fermi}) = \frac{16}{3}\alpha^2 c R_\infty \frac{m_e}{m_\mu}\left[1 + \frac{m_e}{m_\mu}\right]^{-3}. \quad (14)$$

Corrections to this formula have been calculated over the last few decades, with the most recent theoretical work described in [15]. In modern terms, the ground state hyperfine splitting is decomposed into the nonrecoil and recoil contributions of QED diagrams, as well as weak and hadronic contributions. The hyperfine splitting comes mainly from the nonrecoil term, which includes the Fermi term in leading order. The recoil term correction

TABLE I. The sources of uncertainty are outlined in this table. Run dependent errors are added in quadrature before data taken under different running conditions are combined. Errors common to all data sets are then added in quadrature.

Run dependent uncertainties	$\delta\Delta\nu$ [Hz]		$\delta\Delta\nu$ [ppb]		$\delta(\mu_\mu/\mu_p)$ [ppb]	
Sweep mode	H	ν	H	ν	H	ν
Statistical error	89	60	20	13	191	129
Kr density fluctuations	2	2	0.4	0.4	0	0
Drift of Kr density calibration	22	11	4.9	2.5	0	0
Muon stopping distribution	8	5	1.8	1.2	19	17
Magnetic field distribution	0	0	0	0	67	54
Microwave power uncertainty	5	9	1.1	2.0	11	20
Subtotal	92	62	21	14	204	142
Uncertainty in combined results	51		12		117	

Run independent uncertainties	$\delta\Delta\nu$ [Hz]	$\delta\Delta\nu$ [ppb]	$\delta(\mu_\mu/\mu_p)$ [ppb]
Apparatus effect on H field	0	0	30
Absolute calibration of H field	0	0	21
Calibration of Kr density	11	2.5	0
Hydrogen contamination	10	2.2	0
Quadratic pressure shift	8.5	1.9	11
Bloch-Siegert term and nonres. states [19]	2.8	0.6	0
Total common systematic errors	17	3.9	38

contributes about 800 kHz (180 ppm), while the effects of hadronic vacuum polarization and the weak contribution from Z^0 exchange are at the level of 0.250 kHz (56 ppb) and -0.065 kHz (15 ppb), respectively.

Using $\alpha^{-1} = 137.035\,999\,58(52)$ (3.8 ppb) [16,17], $R_\infty = 10\,973\,731.568\,639(91)$ m^{-1} [18], and m_μ/m_e from (13), a value of $\Delta\nu$ can be calculated from the latest theoretical formulation [16]

$$\Delta\nu(\text{theory}) = 4\,463\,302\,563(510)\,(34)(\leq 100)\ \text{Hz}, \quad (15)$$

where the errors, in order, are those from m_μ/m_e, α, and an estimate of the uncertainty from uncalculated terms. Differing estimates of the latter have been made [15]. The fractional difference $[\Delta\nu(\text{exp}) - \Delta\nu(\text{theory})]/\Delta\nu(\text{exp}) = 48 \pm 120$ ppb represents one of the most sensitive tests of the validity of bound state QED.

Alternatively, one may regard the mass ratio m_μ/m_e as a parameter in $\Delta\nu(\text{theory})$ which can be determined by the experimental result $\Delta\nu(\text{exp})$. This yields the ratios $m_\mu/m_e = 206.768\,267\,0(55)$ (27 ppb), and $\mu_\mu/\mu_p = 3.183\,345\,396(94)$ (30 ppb), where we have used α and R_∞ as in (15). Similarly, we can extract a value for the fine structure constant α, using m_μ/m_e from (13), yielding $\alpha^{-1} = 137.035\,996\,3(80)$ (58 ppb).

Significant future improvement in determining μ_μ/μ_p and $\Delta\nu$ would probably require measuring a third transition and/or a new reference standard for the magnetometer, and the use of a more intense pulsed muon source. The latter may be achieved at the Japan Hadron Facility or at the front end of a muon collider.

[1] V. W. Hughes and G. zu Putlitz, in *Quantum Electrodynamics,* edited by T. Kinoshita (World Scientific, Singapore, 1990), p. 822.

[2] H. Grotch and R. A. Hegstrom, Phys. Rev. A **4**, 59 (1971); R. Faustov, Phys. Lett. B **33**, 422 (1970).

[3] R. DeVoe *et al.,* Phys. Rev. Lett. **25**, 1779 (1970).

[4] P. A. Thompson *et al.,* Nucl. Instrum. Methods **161**, 391 (1979); H. W. Reist *et al.,* Nucl. Instrum. Methods **153**, 61 (1978).

[5] D. Ciskowski *et al.,* Nucl. Instrum. Methods Phys. Res., Sect. A **333**, 260 (1993).

[6] C. Caso *et al.,* Eur. Phys. J. **C3**, 1 (1998).

[7] R. Prigl *et al.,* Nucl. Instrum. Methods Phys. Res., Sect. A **374**, 118 (1996).

[8] X. Fei, V. W. Hughes, and R. Prigl, Nucl. Instrum. Methods Phys. Res., Sect. A **394**, 349 (1997), and references therein.

[9] F. G. Mariam *et al.,* Phys. Rev. Lett. **49**, 993 (1982).

[10] M. G. Boshier *et al.,* Phys. Rev. A **52**, 1948 (1995).

[11] W. E. Cleland *et al.,* Phys. Rev. A **5**, 2338 (1972).

[12] D. E. Casperson *et al.,* Phys. Lett. **59B**, 397 (1975); D. Favart *et al.,* Phys. Rev. Lett. **27**, 1340 (1971).

[13] F. J. M. Farley and E. Picasso, in *Quantum Electrodynamics,* edited by T. Kinoshita (World Scientific, Singapore, 1990), p. 479; J. Bailey *et al.,* Nucl. Phys. **B150**, 1 (1979).

[14] E. R. Cohen and B. N. Taylor, Rev. Mod. Phys. **59**, 1121 (1987).

[15] K. Pachucki, Phys. Rev. A **54**, 1994 (1996); S. G. Karshenboim, Z. Phys. D **36**, 11 (1996); S. A. Blundell, K. T. Cheng, and J. Sapirstein, Phys. Rev. Lett. **78**, 4914 (1997); M. Nio and T. Kinoshita, Phys. Rev. D **55**, 7267 (1997); M. I. Eides, H. Grotch, and V. A. Shelyuto, Phys. Rev. D **58**, 013008 (1998).

[16] T. Kinoshita, preprint hep-ph/9808351; T. Kinoshita and M. Nio, in *Frontier Tests of Quantum Electrodynamics and Physics of the Vacuum,* edited by E. Zavattini, D. Bakalov, and C. Rizzo (Heron Press, Sofia, 1998), p. 151, and references therein.

[17] T. Kinoshita, Rep. Prog. Phys. **59**, 1459 (1996); V. W. Hughes and T. Kinoshita, in APS Centennial Volume [Rev. Mod. Phys. (to be published)].

[18] Th. Udem *et al.,* Phys. Rev. Lett. **79**, 2646 (1997).

[19] F. Bloch and A. Siegert, Phys. Rev. **57**, 522 (1940); J. H. Shirley, Phys. Rev. **138**, B979 (1965).